The *kernel-natural stress formulation* constitutive laws

IL Palhares Junior[a,*], JD Evans[d], AM Afonso[b,c]

[a] *Departamento de Matemática e Computação, Faculdade de Ciências e Tecnologia, Universidade Estadual Paulista 'Júlio de Mesquita Filho', 19060-900, Presidente Prudente, São Paulo, Brazil*

[b] *Departamento de Engenharia Mecânica, Centro de Estudos de Fenómenos de Transporte, CEFT, Faculdade de Engenharia da Universidade do Porto, Rua Dr. Roberto Frias s/n, 4200-465, Porto, Portugal.*

[c] *ALiCE, Associate Laboratory in Chemical Engineering, Faculdade de Engenharia, Universidade do Porto, Rua Dr. Roberto Frias s/n, 4200-465 Porto, Portugal*

[d] *Department of Mathematical Sciences, University of Bath, Bath, BA2 7AY, United Kingdom*

Abstract

Keywords: *Kernel-natural* stress transformation, computational rheology

1. Introduction

The natural stress formulation (NSF) has been successfully applied in numerical simulations to compute viscoelastic flows in the presence of singularities in recent years [6, 14, 13, 4]. This approach aligns the polymeric stress tensor along streamlines by employing the velocity field $\mathbf{u}$–tangent to the streamlines–and the normalized gradient of the streamfunction $\frac{\nabla\psi}{|\nabla\psi|^2}$–orthogonal to the streamlines–as the basis for the dyadic decomposition of the stress tensor. This contrasts with the traditional use of the canonical Cartesian basis $\left\{\hat{\boldsymbol{i}}, \hat{\boldsymbol{j}}\right\}$.

The natural basis $\left\{\mathbf{u}, \frac{\nabla\psi}{|\nabla\psi|^2}\right\}$, originally introduced to mitigate downstream instabilities near reentrant corners [22], has proven effective in asymptotic and numerical analyses for accurately capturing stress singularities in reentrant corner flows [7, 12, 5, 8, 13, 4] and in extrudate flows [11, 15, 9, 10]. More recently, Afonso et al. [citation needed] reformulated the NSF as a rotation of the conformation tensor, which is now referred to as the *natural-conformation* formulation. This reformulation enabled the equations of the NSF to be expressed in a fully tensorial format, thereby facilitating its extension to three-dimensional flows.

Despite the success of the natural stress formulation (NSF) in accurately capturing singular behavior in flows with singularities, it is not immune to numerical challenges that also affect

*Corresponding author

Email addresses: irineu.palhares@unesp.br (IL Palhares Junior), masjde@bath.ac.uk (JD Evans), aafonso@fe.up.pt (AM Afonso)

the traditional Cartesian formulation. One significant challenge is the High Weissenberg Number Problem (HWNP), a numerical breakdown that occurs at moderately high Weissenberg numbers. This issue is believed to arise from the limitations of polynomial-based approximations in representing the exponential growth of stresses, particularly in regions of high deformation rates. The problem becomes even more pronounced in flows with singularities or near stagnation points, where the stress gradients are especially steep and difficult to resolve. Furthermore, the manifestation of the HWNP has often been observed to coincide with the loss of positivity of the conformation tensor [19, 21, 1].

To address the challenges posed by the HWNP within the Cartesian formulation, various strategies have been developed over the past decades to preserve the positivity of the conformation tensor. For instance, Collins and Vaithianathan [23] introduced a constitutive model that evolves the eigenvalues and eigenvectors of the conformation tensor, ensuring its positivity. Fattal and Kupferman [17, 18] proposed a widely adopted approach involving the application of the natural logarithm to the conformation tensor, effectively mitigating steep gradients. Similarly, Balci et al. [2] suggested a square-root decomposition of the conformation tensor, which also maintains its positivity. Expanding on these concepts, Afonso et al. [1] developed a generalized framework using a kernel function. This approach encompasses any transformation that is invertible, differentiable, and continuous, enabling its application to a broad range of matrix transformations.

To mitigate the HWNP within the natural formulation, this work proposes applying the kernel approach introduced by Afonso et al. [1] to the *natural-conformation* equations. Specifically, we present the governing equations for the *kernel-natural* stress conformation and analyze the performance of two kernel transformations: the natural logarithm and square-root. These transformations are evaluated in two benchmark problems: the 4:1 contraction flow and the confined flow around a cylinder. These cases were selected due to their distinct challenges–singularities in the former and stagnation points in the latter–making them ideal scenarios for testing the *kernel-natural* formulation capabilities.

2. Governing equations

The governing equations for incompressible viscoelastic flows consist of the conservation of momentum:

$$Re\frac{D\mathbf{u}}{Dt} = -\nabla p + 2\beta\nabla^2\mathbf{u} + \nabla\cdot\boldsymbol{\tau},$$

the conservation of mass:

$$\nabla\cdot\mathbf{u} = 0,$$

and the Oldroyd-B constitutive equation for the polymer stress tensor $\boldsymbol{\tau}$:

$$\boldsymbol{\tau} + Wi\overset{\triangledown}{\boldsymbol{\tau}} = 2\,(1-\beta)\,\mathbf{D},$$

where $\mathbf{u}$ is the velocity field, p is the pressure, and $\mathbf{D} = \frac{1}{2}(\nabla\mathbf{u} + (\nabla\mathbf{u})^\top)$ is the rate-of-strain tensor. Here, Re is the Reynolds number, Wi is the Weissenberg number, and β is the ratio of solvent viscosity η_s to the total viscosity $(\eta_s + \eta_p)$. The upper convected derivative of $\boldsymbol{\tau}$ is given by:

$$\overset{\triangledown}{\boldsymbol{\tau}} = \frac{\partial \boldsymbol{\tau}}{\partial t} + (\mathbf{u} \cdot \nabla)\boldsymbol{\tau} - \boldsymbol{\tau} \cdot \nabla \mathbf{u} - (\nabla \mathbf{u})^\top \cdot \boldsymbol{\tau}.$$

Traditionally, the polymer stress tensor $\boldsymbol{\tau}$ is expressed in the Cartesian basis $\{\hat{\mathbf{i}}, \hat{\mathbf{j}}\}$, leading to:

$$\boldsymbol{\tau} = \hat{\mathbf{i}}\hat{\mathbf{i}}^\top \tau_{xx} + (\hat{\mathbf{i}}\hat{\mathbf{j}}^\top + \hat{\mathbf{j}}\hat{\mathbf{i}}^\top)\tau_{xy} + \hat{\mathbf{j}}\hat{\mathbf{j}}^\top \tau_{yy}.$$

Alternatively, Renardy [22] proposed aligning the stress tensor with the flow streamlines by using a natural basis $\{\hat{\mathbf{u}} = \mathbf{u}, \quad \hat{\mathbf{v}} = \frac{(-v,u)}{|\mathbf{u}|^2}\}$, i.e.,

$$\boldsymbol{\tau} = \hat{\mathbf{u}}\hat{\mathbf{u}}^\top \lambda + \left(\hat{\mathbf{u}}\hat{\mathbf{v}}^\top + \hat{\mathbf{v}}\hat{\mathbf{u}}^\top\right)\mu + \hat{\mathbf{v}}\hat{\mathbf{v}}^\top \nu,$$

where λ, μ and ν are the natural stresses. Building on this, Evans et al. [5] proposed a related formulation, where the conformation tensor $\mathbf{A}$– a variance-covariance and symmetric positive definite tensor (SPD)– was expanded in the natural basis instead of the stress tensor:

$$\mathbf{A} = \hat{\mathbf{u}}\hat{\mathbf{u}}^\top \lambda + \left(\hat{\mathbf{u}}\hat{\mathbf{v}}^\top + \hat{\mathbf{v}}\hat{\mathbf{u}}^\top\right)\mu + \hat{\mathbf{v}}\hat{\mathbf{v}}^\top \nu. \tag{1}$$

The conformation tensor $\mathbf{A}$ is related to the extra-stress tensor $\boldsymbol{\tau}$ via:

$$\boldsymbol{\tau} = \frac{1-\beta}{Wi}\left(\mathbf{A} - \mathbf{I}\right),$$

where $\mathbf{I}$ is the identity tensor. This formulation proves particularly advantageous in asymptotic analyses, such as boundary layer equations in viscoelastic flows around reentrant corners, where the identity tensor $\mathbf{I}$ plays a pivotal role [5].

Afonso et al. later reformulated this approach into the natural conformation framework. They introduced the natural conformation tensor $\mathbf{N}$, defined as a rotation of the conformation tensor:

$$\mathbf{N} = \mathbf{R}^\top \mathbf{A} \mathbf{R},$$

where the rotation matrix $\mathbf{R}$ is:

$$\mathbf{R} = \frac{1}{|\mathbf{u}|}\begin{pmatrix} u & -v \\ v & u \end{pmatrix}.$$

This transformation results in a tensorial equation for $\mathbf{N}$:

$$\frac{D\mathbf{N}}{Dt} = \mathbf{N}\widetilde{\nabla \mathbf{u}} + \widetilde{\nabla \mathbf{u}}^\top \mathbf{N} + \frac{1}{Wi}(\mathbf{N} - \mathbf{I}), \tag{2}$$

where $\widetilde{\nabla \mathbf{u}} = \mathbf{R}^\top \nabla \mathbf{u} \mathbf{R} - \mathbf{H}$, and $\mathbf{H} = \mathbf{R}\frac{D\mathbf{R}^\top}{Dt}$ is a skew-symmetric tensor.

Although the natural-conformation formulation addresses downstream instabilities in reentrant corner flows [22], it remains susceptible to the HWNP. Stabilization techniques are thus required to mitigate these issues. Given that $\mathbf{N}$ is symmetric and positive definite, established methods like the log-conformation [17] and square-root decomposition [2] can be applied effectively.

In the next section, we introduce the kernel stabilization strategy developed by Afonso et al. [1], which generalizes these approaches by defining a generic kernel function to stabilize the natural conformation equations.

3. The kernel-natural stress formulation

Following the work of Fattal and Kupferman [17], the tensor $\widetilde{\nabla \mathbf{u}}^T$ can be decomposed as

$$\widetilde{\nabla \mathbf{u}}^T = \mathbf{\Omega} + \mathbf{B} + \mathbf{S}\mathbf{N}^{-1},$$

where $\mathbf{\Omega}$ and $\mathbf{S}$ are antisymmetric matrices, while $\mathbf{B}$ is a symmetric matrix that commutes with $\mathbf{N}$.

Substituting this decomposition into Eq. (2), the evolution equation for $\mathbf{N}$ becomes

$$\frac{D\mathbf{N}}{Dt} = \mathbf{\Omega}\mathbf{N} - \mathbf{N}\mathbf{\Omega} + 2\mathbf{B}\mathbf{N} + \frac{1}{Wi}\left(\mathbf{N} - \mathbf{I}\right),$$

which is consistent with the formulation proposed by Fattal and Kupferman [17].

Since $\mathbf{N}$ is symmetric and positive definite, it can be decomposed into its eigenvalues and eigenvectors:

$$\mathbf{N} = \mathbf{O}\mathbf{\Lambda}\mathbf{O}^T,$$

where $\mathbf{O}$ is an orthogonal matrix whose columns are the eigenvectors, and $\mathbf{\Lambda}$ is a diagonal matrix containing the eigenvalues. Applying the total derivative to $\mathbf{\Lambda} = \mathbf{O}^T\mathbf{N}\mathbf{O}$, we obtain

$$\frac{D\mathbf{\Lambda}}{Dt} = \frac{D\mathbf{O}^T}{Dt}\mathbf{N}\mathbf{O} + \mathbf{O}^T\frac{D\mathbf{N}}{Dt}\mathbf{O} + \mathbf{O}^T\mathbf{N}\frac{D\mathbf{O}}{Dt}.$$

Using Eq. (2), the evolution equation for $\mathbf{\Lambda}$ becomes

$$\frac{D\mathbf{\Lambda}}{Dt} = \mathbf{\Lambda}\mathbf{P} - \mathbf{P}\mathbf{\Lambda} + \widetilde{\mathbf{\Omega}}\mathbf{\Lambda} - \mathbf{\Lambda}\widetilde{\mathbf{\Omega}} + 2\widetilde{\mathbf{B}}\mathbf{\Lambda} + \frac{1}{Wi}\left(\mathbf{\Lambda} - \mathbf{I}\right), \tag{3}$$

where $\mathbf{P} = \mathbf{O}^T\frac{D\mathbf{O}}{Dt} = -\frac{D\mathbf{O}^T}{Dt}\mathbf{O} = -\mathbf{P}^T$, $\widetilde{\mathbf{\Omega}} = \mathbf{O}^T\mathbf{\Omega}\mathbf{O}$, and $\widetilde{\mathbf{B}} = \mathbf{O}^T\mathbf{B}\mathbf{O}$. Since both $\mathbf{P}$ and $\widetilde{\mathbf{\Omega}}$ are antisymmetric, they do not influence the evolution of $\mathbf{\Lambda}$. Thus, Eq. (3) simplifies to two separate equations:

$$\begin{cases} \dfrac{D\mathbf{\Lambda}}{Dt} = 2\widetilde{\mathbf{B}}\mathbf{\Lambda} + \dfrac{1}{Wi}\left(\mathbf{\Lambda} - \mathbf{I}\right), \\ \mathbf{\Lambda}\mathbf{P} - \mathbf{P}\mathbf{\Lambda} = \mathbf{\Lambda}\widetilde{\mathbf{\Omega}} - \widetilde{\mathbf{\Omega}}\mathbf{\Lambda}. \end{cases} \tag{4}$$

The second equation implies $\mathbf{P} = \widetilde{\mathbf{\Omega}}$.

The kernel-natural conformation formulation is introduced by defining the kernel transformation as

$$\mathbb{K}\left(\mathbf{N}\right) = \mathbf{O}\mathbb{K}\left(\mathbf{\Lambda}\right)\mathbf{O}^T, \tag{5}$$

where $\mathbb{K}\left(\ \right)$ is any continuous, invertible, and differentiable matrix transformation. From the first equation in (4), we can define $\frac{D\mathbb{K}(\mathbf{\Lambda})}{Dt} = \frac{D\mathbf{\Lambda}}{Dt}\frac{\partial\mathbb{K}(\mathbf{\Lambda})}{\partial\mathbf{\Lambda}}$ as

$$\frac{D\mathbb{K}\left(\mathbf{\Lambda}\right)}{Dt} = \left[2\widetilde{\mathbf{B}}\mathbf{\Lambda} + \frac{1}{Wi}\left(\mathbf{\Lambda} - \mathbf{I}\right)\right]\mathbf{J}, \tag{6}$$

where $\mathbf{J} = \frac{\partial \mathbb{K}(\mathbf{\Lambda})}{\partial \mathbf{\Lambda}}$. Applying the chain rule to Eq. (5) and substituting Eq. (6) leads to

$$\frac{D\mathbb{K}\left(\mathbf{N}\right)}{Dt} = \mathbf{\Omega}\mathbb{K}\left(\mathbf{N}\right) - \mathbb{K}\left(\mathbf{N}\right)\mathbf{\Omega} + \left[2\mathbf{B}\mathbf{N} + \frac{1}{Wi}\left(\mathbf{N} - \mathbf{I}\right)\right]\widetilde{\mathbf{J}},$$

where $\widetilde{\mathbf{J}} = \mathbf{O}\mathbf{J}\mathbf{O}^T$.

For simplicity, we focus on two kernel transformations: the natural logarithm and square-root, defined respectively as

$$\begin{cases} \ln \mathbf{N} = \mathbf{O}\ln\mathbf{\Lambda}\mathbf{O}^T = \mathbf{O}\begin{pmatrix} \ln\lambda_1 & 0 \\ 0 & \ln\lambda_2 \end{pmatrix}\mathbf{O}^T, \\ \sqrt{\mathbf{N}} = \mathbf{O}\sqrt{\mathbf{\Lambda}}\mathbf{O}^T = \mathbf{O}\begin{pmatrix} \sqrt{\lambda_1} & 0 \\ 0 & \sqrt{\lambda_2} \end{pmatrix}\mathbf{O}. \end{cases}$$

4. Numerical results

In order to analyze the *kernel-natural* conformation performance, we selected two benchmark flow cases: 4:1 planar contraction and a confined cylinder. These problems were selected because they are simple in geometry, but they are numerically challenging due their singularity in the 4:1 planar contraction and stagnation points in the cylinder flow.

4.1. Flow in a 4:1 planar contraction

The geometry and some features of the 4:1 planar contraction flow are depicted in Fig. 1. The downstream channel width is $2L$, while the upstream channel width is $8L$. Both channels length, upstream and downstream of the 4:1 planar contraction, are $100L$. A uniform velocity prof

The contraction simulations were performed using $\beta = \frac{1}{9}$ at low Reynolds number flow condition, $Re = 0.01$, considering some values of the Weissenberg number, $Wi = 0.5, 1, 5, 10$. The critical Weissenberg number, where the standard extra-stress tensor formulation diverges, for the Oldroyd-B fluid in a 4:1 planar contraction is some value between 1.5 and 2.8 (see [3, 24])

1-Colocar resultados dos slopes Figure 2

2-Resultados da positividade do tensor N.

4.2. Flow around a confined cylinder

The critical Weissenberg number for the confined cylinder flow is some value bellow 1 (see [1, 16, 20]).

1-Resultados sobre a diferenÃ§a de tensÃ$\mu esnormais 2 - Resultados da positivdade de N$.

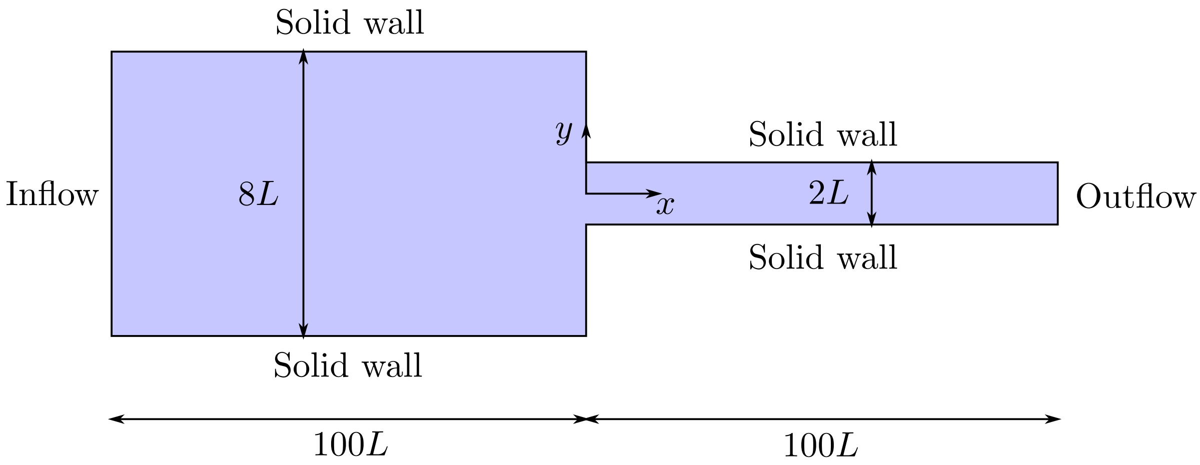

Figure 1: Geometry of the 4:1 contraction flow.

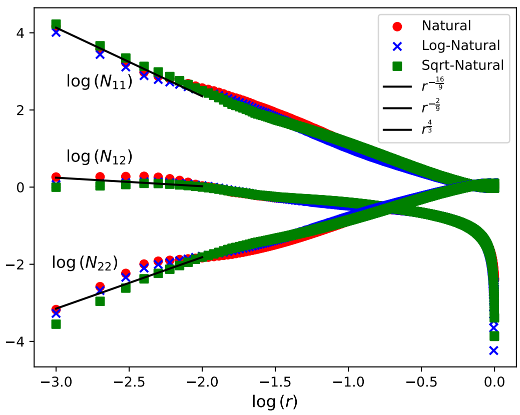

Figure 2: Caption

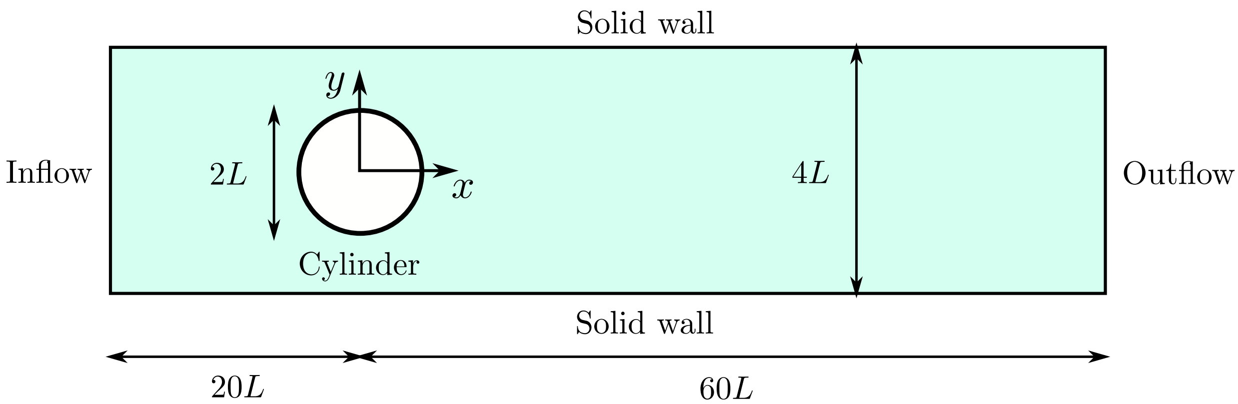

5. Conclusions

References

[1] A.M. Afonso, F.T. Pinho, and M.A. Alves. "The kernel-conformation constitutive laws". In: *Journal of Non-Newtonian Fluid Mechanics* Not available (Oct. 2011), Not available. ISSN: 0377-0257. DOI: 10.1016/j.jnnfm.2011.09.008. URL: https://dx.doi.org/10.1016/j.jnnfm.2011.09.008.

[2] Nusret Balci et al. “Symmetric factorization of the conformation tensor in viscoelastic fluid models”. In: *Journal of Non-Newtonian Fluid Mechanics* 166.11 (2011), pp. 546–553.

[3] Xingyuan Chen et al. “A comparison of stabilisation approaches for finite-volume simulation of viscoelastic fluid flow”. In: *International Journal of Computational Fluid Dynamics* 27.6-7 (2013), pp. 229–250.

[4] Jonathan David et al. “Numerical verification of sharp corner behavior for Giesekus and Phan-Thien–Tanner fluids”. In: *Physics of Fluids* 34.11 (2022).

[5] J.D. Evans. “Re-entrant corner behaviour of the Giesekus fluid with a solvent viscosity”. In: *Journal of Non-Newtonian Fluid Mechanics* 165 (May 2010), pp. 538–543. ISSN: 0377-0257. DOI: `10.1016/j.jnnfm.2010.01.010`. URL: `https://dx.doi.org/10.1016/j.jnnfm.2010.01.010`.

[6] J.D. Evans and C.M. Oishi. “Transient computations using the natural stress formulation for solving sharp corner flows”. In: *Journal of Non-Newtonian Fluid Mechanics* 249 (Nov. 2017), pp. 48–52. ISSN: 0377-0257. DOI: `10.1016/j.jnnfm.2017.08.012`. URL: `https://dx.doi.org/10.1016/j.jnnfm.2017.08.012`.

[7] JD Evans. “Re-entrant corner flows of UCM fluids: The natural stress basis”. In: *Journal of non-newtonian fluid mechanics* 150.2-3 (2008), pp. 139–153.

[8] Jonathan D Evans. “Re-entrant corner behaviour of the PTT fluid with a solvent viscosity”. In: *Journal of non-newtonian fluid mechanics* 165.9-10 (2010), pp. 527–537.

[9] Jonathan D Evans and Morgan L Evans. “Stress boundary layers for the Giesekus fluid at the static contact line in extrudate swell”. In: *AIMS Mathematics* 9.11 (2024), pp. 32921–32944.

[10] Jonathan D Evans and Morgan L Evans. “Stress boundary layers for the Phan-Thien–Tanner fluid at the static contact line in extrudate swell”. In: *Journal of Engineering Mathematics* 150.1 (2025), pp. 1–23.

[11] Jonathan D Evans and Morgan L Evans. “The extrudate swell singularity of Phan-Thien–Tanner and Giesekus fluids”. In: *Physics of Fluids* 31.11 (2019).

[12] Jonathan D Evans and David N Sibley. “Re-entrant corner flow for PTT fluids in the natural stress basis”. In: *Journal of non-newtonian fluid mechanics* 157.1-2 (2009), pp. 79–91.

[13] Jonathan D Evans et al. “Testing viscoelastic numerical schemes using the Oldroyd-B fluid in Newtonian kinematics”. In: *Applied Mathematics and Computation* 387 (2020), p. 125106.

[14] Jonathan David Evans et al. “Numerical study of the stress singularity in stick-slip flow of the Phan-Thien Tanner and Giesekus fluids”. In: *Physics of Fluids* 31.9 (2019).

[15] Morgan Evans. *The Extrudate Swell Singularity of Viscoelastic Fluids*. University of Bath (United Kingdom), 2020.

[16] Yurun Fan, Roger I Tanner, and Nhan Phan-Thien. “Galerkin/least-square finite-element methods for steady viscoelastic flows”. In: *Journal of Non-Newtonian Fluid Mechanics* 84.2-3 (1999), pp. 233–256.

[17] Raanan Fattal and Raz Kupferman. “Constitutive laws for the matrix-logarithm of the conformation tensor”. In: *Journal of Non-Newtonian Fluid Mechanics* 123 (Nov. 2004), pp. 281–285. ISSN: 0377-0257. DOI: `10.1016/j.jnnfm.2004.08.008`. URL: `https://dx.doi.org/10.1016/j.jnnfm.2004.08.008`.

[18] Raanan Fattal and Raz Kupferman. “Time-dependent simulation of viscoelastic flows at high Weissenberg number using the log-conformation representation”. In: *Journal of Non-Newtonian Fluid Mechanics* 126.1 (2005), pp. 23–37.

[19] MA Hulsen, APG Van Heel, and BHAA Van Den Brule. “Simulation of viscoelastic flows using Brownian configuration fields”. In: *Journal of Non-Newtonian Fluid Mechanics* 70.1-2 (1997), pp. 79–101.

[20] Paulo J Oliveira and Amílcar IP Miranda. “A numerical study of steady and unsteady viscoelastic flow past bounded cylinders”. In: *Journal of non-Newtonian fluid mechanics* 127.1 (2005), pp. 51–66.

[21] Timothy Nigel Phillips and AJ Williams. “Comparison of creeping and inertial flow of an Oldroyd B fluid through planar and axisymmetric contractions”. In: *Journal of Non-Newtonian Fluid Mechanics* 108.1-3 (2002), pp. 25–47.

[22] M. Renardy. “How to integrate the upper convected Maxwell (UCM) stresses near a singularity (and maybe elsewhere, too)”. In: *Journal of Non-Newtonian Fluid Mechanics* 52 (Apr. 1994), pp. 91–95. ISSN: 0377-0257. DOI: 10.1016/0377-0257(94)85060-7. URL: https://dx.doi.org/10.1016/0377-0257(94)85060-7.

[23] T Vaithianathan and Lance R Collins. “Numerical approach to simulating turbulent flow of a viscoelastic polymer solution”. In: *Journal of Computational Physics* 187.1 (2003), pp. 1–21.

[24] K Walters and MF Webster. “The distinctive CFD challenges of computational rheology”. In: *International journal for numerical methods in fluids* 43.5 (2003), pp. 577–596.